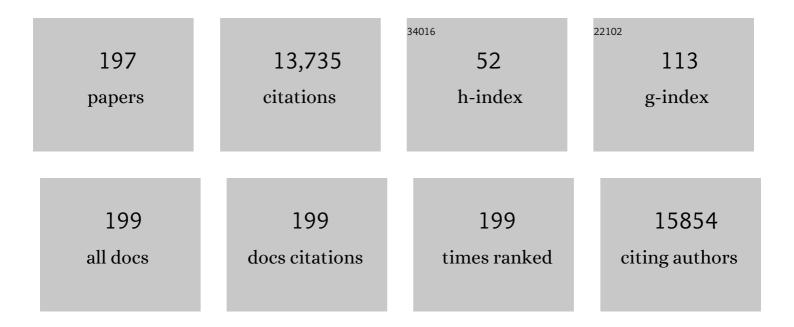
Dattatray J Late

List of Publications by Year in descending order

Source: https://exaly.com/author-pdf/8620948/publications.pdf Version: 2024-02-01



#	Article	IF	CITATIONS
1	MoS ₂ and WS ₂ Analogues of Graphene. Angewandte Chemie - International Edition, 2010, 49, 4059-4062.	7.2	1,417
2	Sensing Behavior of Atomically Thin-Layered MoS ₂ Transistors. ACS Nano, 2013, 7, 4879-4891.	7.3	1,158
3	Hysteresis in Single-Layer MoS ₂ Field Effect Transistors. ACS Nano, 2012, 6, 5635-5641.	7.3	956
4	GaS and GaSe Ultrathin Layer Transistors. Advanced Materials, 2012, 24, 3549-3554.	11.1	580
5	Rapid Characterization of Ultrathin Layers of Chalcogenides on SiO ₂ /Si Substrates. Advanced Functional Materials, 2012, 22, 1894-1905.	7.8	436
6	Recent developments in 2D layered inorganic nanomaterials for sensing. Nanoscale, 2015, 7, 13293-13312.	2.8	386
7	Band-like transport in high mobility unencapsulated single-layer MoS2 transistors. Applied Physics Letters, 2013, 102, .	1.5	359
8	Single-layer MoSe2 based NH3 gas sensor. Applied Physics Letters, 2014, 105, .	1.5	326
9	Humidity Sensing and Photodetection Behavior of Electrochemically Exfoliated Atomically Thin-Layered Black Phosphorus Nanosheets. ACS Applied Materials & Interfaces, 2016, 8, 11548-11556.	4.0	274
10	Thermal Expansion, Anharmonicity and Temperatureâ€Dependent Raman Spectra of Single―and Few‣ayer MoSe ₂ and WSe ₂ . ChemPhysChem, 2014, 15, 1592-1598.	1.0	242
11	Highly Transparent Wafer-Scale Synthesis of Crystalline WS ₂ Nanoparticle Thin Film for Photodetector and Humidity-Sensing Applications. ACS Applied Materials & Interfaces, 2016, 8, 3359-3365.	4.0	226
12	Superior Field Emission Properties of Layered WS2-RGO Nanocomposites. Scientific Reports, 2013, 3, 3282.	1.6	218
13	Enhanced Fieldâ€Emission Behavior of Layered MoS ₂ Sheets. Small, 2013, 9, 2730-2734.	5.2	196
14	Freestanding Borophene and Its Hybrids. Advanced Materials, 2019, 31, e1900353.	11.1	195
15	Temperature Dependent Phonon Shifts in Single-Layer WS ₂ . ACS Applied Materials & Interfaces, 2014, 6, 1158-1163.	4.0	188
16	Large area chemical vapor deposition of monolayer transition metal dichalcogenides and their temperature dependent Raman spectroscopy studies. Nanoscale, 2016, 8, 3008-3018.	2.8	186
17	Temperature dependent Raman spectroscopy of chemically derived few layer MoS2 and WS2 nanosheets. Applied Physics Letters, 2014, 104, .	1.5	180
18	Liquid exfoliation of black phosphorus nanosheets and its application as humidity sensor. Microporous and Mesoporous Materials, 2016, 225, 494-503.	2.2	177

#	Article	IF	CITATIONS
19	Pulsed Laser-Deposited MoS ₂ Thin Films on W and Si: Field Emission and Photoresponse Studies. ACS Applied Materials & Interfaces, 2014, 6, 15881-15888.	4.0	169
20	A study of the synthetic methods and properties of graphenes. Science and Technology of Advanced Materials, 2010, 11, 054502.	2.8	164
21	NO ₂ and humidity sensing characteristics of few-layer graphenes. Journal of Experimental Nanoscience, 2009, 4, 313-322.	1.3	154
22	Temperature Dependent Phonon Shifts in Few-Layer Black Phosphorus. ACS Applied Materials & Interfaces, 2015, 7, 5857-5862.	4.0	153
23	2D layered transition metal dichalcogenides (MoS2): Synthesis, applications and theoretical aspects. Applied Materials Today, 2018, 13, 242-270.	2.3	139
24	ZnO Multipods, Submicron Wires, and Spherical Structures and Their Unique Field Emission Behavior. Journal of Physical Chemistry B, 2006, 110, 18236-18242.	1.2	136
25	Graphene quantum dots as enhanced plant growth regulators: effects on coriander and garlic plants. Journal of the Science of Food and Agriculture, 2015, 95, 2772-2778.	1.7	126
26	Ultra-thin V ₂ O ₅ nanosheet based humidity sensor, photodetector and its enhanced field emission properties. RSC Advances, 2015, 5, 88796-88804.	1.7	112
27	Electrodeposited Nickel Cobalt Manganese based mixed sulfide nanosheets for high performance supercapacitor application. Microporous and Mesoporous Materials, 2017, 244, 101-108.	2.2	110
28	Enhanced field emission properties of doped graphene nanosheets with layered SnS2. Applied Physics Letters, 2014, 105, .	1.5	109
29	SnS ₂ nanoflakes for efficient humidity and alcohol sensing at room temperature. RSC Advances, 2016, 6, 105421-105427.	1.7	100
30	Temperature-Dependent Raman Spectroscopy of Titanium Trisulfide (TiS ₃) Nanoribbons and Nanosheets. ACS Applied Materials & Interfaces, 2015, 7, 24185-24190.	4.0	89
31	Electrochemically Exfoliated Black Phosphorus Nanosheets – Prospective Field Emitters. European Journal of Inorganic Chemistry, 2015, 2015, 3102-3107.	1.0	87
32	Ultralow threshold field emission from a single multipod structure of ZnO. Applied Physics Letters, 2006, 88, 042107.	1.5	85
33	Superior humidity sensor and photodetector of mesoporous ZnO nanosheets at room temperature. Sensors and Actuators B: Chemical, 2019, 293, 83-92.	4.0	84
34	Field emission studies of novel ZnO nanostructures in high and low field regions. Nanotechnology, 2006, 17, 2730-2735.	1.3	80
35	Oxidative and membrane stress-mediated antibacterial activity of WS ₂ and rGO-WS ₂ nanosheets. RSC Advances, 2015, 5, 74726-74733.	1.7	80
36	Recent developments in self-powered smart chemical sensors for wearable electronics. Nano Research, 2021, 14, 3669-3689.	5.8	78

#	Article	IF	CITATIONS
37	Hydrothermal growth of MoSe2 nanoflowers for photo- and humidity sensor applications. Sensors and Actuators A: Physical, 2019, 295, 160-168.	2.0	76
38	Facile Production of Mesoporous WO ₃ -rGO Hybrids for High-Performance Supercapacitor Electrodes: An Experimental and Computational Study. ACS Sustainable Chemistry and Engineering, 2019, 7, 2350-2359.	3.2	75
39	Electrochemical synthesis of a ternary transition metal sulfide nanosheets on nickel foam and energy storage application. Journal of Alloys and Compounds, 2017, 695, 154-161.	2.8	73
40	Microwave and hydrothermal syntheses of WSe ₂ micro/nanorods and their application in supercapacitors. RSC Advances, 2015, 5, 21700-21709.	1.7	72
41	Temperature effects on the Raman spectra of graphenes: dependence on the number of layers and doping. Journal of Physics Condensed Matter, 2011, 23, 055303.	0.7	71
42	High performance humidity sensor and photodetector based on SnSe nanorods. Materials Research Express, 2016, 3, 105038.	0.8	62
43	Electronic structure and properties of layered gallium telluride. Chemical Physics Letters, 2016, 651, 148-154.	1.2	62
44	A combined experimental and theoretical study of the structural, electronic and vibrational properties of bulk and few-layer Td-WTe ₂ . Journal of Physics Condensed Matter, 2015, 27, 285401.	0.7	61
45	Characteristics of field-effect transistors based on undoped and B- and N-doped few-layer graphenes. Solid State Communications, 2010, 150, 734-738.	0.9	60
46	MoO3-rGO nanocomposites for electrochemical energy storage. Applied Surface Science, 2017, 418, 2-8.	3.1	60
47	Enhanced field emission of plasma treated multilayer graphene. Applied Physics Letters, 2015, 107, .	1.5	58
48	Field emission studies of pulsed laser deposited films on W and Re. Ultramicroscopy, 2007, 107, 825-832.	0.8	56
49	Room-temperature gas sensors based on gallium nitride nanoparticles. Solid State Communications, 2010, 150, 2053-2056.	0.9	56
50	High-Performance Sensing Behavior Using Electronic Ink of 2D SnSe ₂ Nanosheets. ChemistrySelect, 2017, 2, 4068-4075.	0.7	56
51	Phase transformation in tungsten oxide nanoplates as a function of post-annealing temperature and its electrochemical influence on energy storage. Nanoscale Advances, 2020, 2, 4689-4701.	2.2	56
52	Field emission properties of spinel ZnCo ₂ O ₄ microflowers. RSC Advances, 2015, 5, 5372-5378.	1.7	55
53	Large area, broadband and highly sensitive photodetector based on ZnO-WS2/Si heterojunction. Solar Energy, 2020, 206, 974-982.	2.9	53
54	Field emission studies on well adhered pulsed laser deposited LaB6 on W tip. Applied Physics Letters, 2006, 89, 123510.	1.5	52

#	Article	IF	CITATIONS
55	Pt-nanoparticle functionalized carbon nano-onions for ultra-high energy supercapacitors and enhanced field emission behaviour. RSC Advances, 2015, 5, 80990-80997.	1.7	52
56	Metallic Few‣ayer Flowerlike VS ₂ Nanosheets as Field Emitters. European Journal of Inorganic Chemistry, 2014, 2014, 5331-5336.	1.0	51
57	Field emission properties of ZnO nanosheet arrays. Applied Physics Letters, 2014, 105, .	1.5	51
58	Recent advances in 2D black phosphorus based materials for gas sensing applications. Journal of Materials Chemistry C, 2021, 9, 3773-3794.	2.7	51
59	Ultra-fast α-MoO3 nanorod-based Humidity sensor. International Journal of Higher Education Management, 2016, 2, 15-22.	1.0	50
60	Highly sensitive and flexible pressure sensor based on two-dimensional MoSe2 nanosheets for online wrist pulse monitoring. Journal of Colloid and Interface Science, 2021, 584, 495-504.	5.0	49
61	Photosensitive WS ₂ /ZnO Nano-Heterostructure-Based Electrocatalysts for Hydrogen Evolution Reaction. ACS Applied Energy Materials, 2021, 4, 755-762.	2.5	49
62	Plasmon-enhanced photoresponse in Ag-WS2/Si heterojunction. Applied Surface Science, 2021, 538, 148121.	3.1	48
63	A Semiconducting Organic Radical Cationic Host–Guest Complex. ACS Nano, 2012, 6, 9964-9971.	7.3	47
64	Negative infrared photocurrent response in layered WS2/reduced graphene oxide hybrids. Applied Physics Letters, 2014, 105, .	1.5	46
65	Synthesis of orthorhombic-molybdenum trioxide (α-MoO3) thin films by hot wire-CVD and investigations of its humidity sensing properties. Journal of Materials Science: Materials in Electronics, 2017, 28, 15790-15796.	1.1	44
66	Optimized performance of nickel in crystal-layered arrangement of NiFe2O4/rGO hybrid for high-performance oxygen evolution reaction. International Journal of Hydrogen Energy, 2021, 46, 2617-2629.	3.8	44
67	Reduction of graphene oxide by 100 MeV Au ion irradiation and its application as H ₂ O ₂ sensor. Journal Physics D: Applied Physics, 2015, 48, 365105.	1.3	43
68	Enhanced energy density and stability of self-assembled cauliflower of Pd doped monoclinic WO3 nanostructure supercapacitor. Materials Chemistry and Physics, 2019, 225, 192-199.	2.0	42
69	Enhanced field emission from LaB6 thin films with nanoprotrusions grown by pulsed laser deposition on Zr foil. Applied Surface Science, 2008, 254, 3601-3605.	3.1	41
70	Nanostructured 2D MoS ₂ honeycomb and hierarchical 3D CdMoS ₄ marigold nanoflowers for hydrogen production under solar light. Journal of Materials Chemistry A, 2015, 3, 21233-21243.	5.2	41
71	Temperature dependent Raman spectroscopy of electrochemically exfoliated few layer black phosphorus nanosheets. RSC Advances, 2016, 6, 76551-76555.	1.7	40
72	Graphene nanoribbons as prospective field emitter. Applied Physics Letters, 2015, 106, 023111.	1.5	39

#	Article	IF	CITATIONS
73	Spectral analysis of the emission current noise exhibited by few layer WS2 nanosheets emitter. Ultramicroscopy, 2015, 149, 51-57.	0.8	39
74	Laser exfoliation of 2D black phosphorus nanosheets and their application as a field emitter. RSC Advances, 2016, 6, 112103-112108.	1.7	39
75	Negative axicon tip-based fiber optic interferometer cavity sensor for volatile gas sensing. Optics Express, 2019, 27, 7277.	1.7	37
76	Sb-doped SnO2 wire: Highly stable field emitter. Journal of Crystal Growth, 2007, 307, 87-91.	0.7	36
77	High current density, low threshold field emission from functionalized carbon nanotube bucky paper. Applied Physics Letters, 2010, 97, .	1.5	35
78	Temperature Dependent Raman Spectroscopy and Sensing Behavior of Few Layer SnSe ₂ Nanosheets. ChemistrySelect, 2016, 1, 5380-5387.	0.7	35
79	2D-MoS ₂ nanosheets as effective hole transport materials for colloidal PbS quantum dot solar cells. Nanoscale Advances, 2019, 1, 1387-1394.	2.2	35
80	Morphology and crystal structure dependent pseudocapacitor performance of hydrated WO ₃ nanostructures. Materials Advances, 2020, 1, 2492-2500.	2.6	35
81	Molecular charge-transfer interaction with single-layer graphene. Journal of Experimental Nanoscience, 2011, 6, 641-651.	1.3	34
82	Facile synthesis of Ag nanowire–rGO composites and their promising field emission performance. RSC Advances, 2015, 5, 41887-41893.	1.7	34
83	Enhanced field emission from pulsed laser deposited nanocrystalline ZnO thin films on Re andÂW. Applied Physics A: Materials Science and Processing, 2009, 95, 613-620.	1.1	33
84	3D Hetero-architecture of GdB ₆ nanoparticles on lessened cubic Cu ₂ O nanowires: enhanced field emission behaviour. CrystEngComm, 2015, 17, 3936-3944.	1.3	33
85	Synthesis of Ni-doped ZnO nanostructures by low-temperature wet chemical method and their enhanced field emission properties. RSC Advances, 2016, 6, 104318-104324.	1.7	33
86	Pressure-Induced Phase Transitions in Germanium Telluride: Raman Signatures of Anharmonicity and Oxidation. Physical Review Letters, 2019, 122, 145701.	2.9	33
87	Temperature-dependent Raman spectroscopy and sensor applications of PtSe ₂ nanosheets synthesized by wet chemistry. Beilstein Journal of Nanotechnology, 2019, 10, 467-474.	1.5	33
88	Exfoliation of Bulk Inorganic Layered Materials into Nanosheets by the Rapid Quenching Method and Their Electrochemical Performance. European Journal of Inorganic Chemistry, 2015, 2015, 1973-1980.	1.0	32
89	Comparative Study of Cold Electron Emission from 2D Ti ₃ C ₂ T _X MXene Nanosheets with Respect to Its Precursor Ti ₃ SiC ₂ MAX Phase. ACS Applied Electronic Materials, 2022, 4, 2656-2666.	2.0	32
90	Thickness tunable transport in alloyed WSSe field effect transistors. Applied Physics Letters, 2016, 109, .	1.5	31

#	Article	IF	CITATIONS
91	Enhanced field emission behavior of layered MoSe ₂ . Materials Research Express, 2016, 3, 035003.	0.8	31
92	VSe2-reduced graphene oxide as efficient cathode material for field emission. Journal of Physics and Chemistry of Solids, 2019, 128, 384-390.	1.9	31
93	Enhanced energy storage performance and theoretical studies of 3D cuboidal manganese diselenides embedded with multiwalled carbon nanotubes. Journal of Colloid and Interface Science, 2021, 598, 500-510.	5.0	31
94	Some aspects of pulsed laser deposited nanocrystalline LaB ₆ film: atomic force microscopy, constant force current imaging and field emission investigations. Nanotechnology, 2008, 19, 265605.	1.3	30
95	Highly efficient field emission properties of radially aligned carbon nanotubes. Journal of Materials Chemistry C, 2018, 6, 6584-6590.	2.7	30
96	Temperature driven high-performance pseudocapacitor of carbon nano-onions supported urchin like structures of α-MnO2 nanorods. Electrochimica Acta, 2020, 354, 136626.	2.6	30
97	Field emission applications of graphene-analogous two-dimensional materials: recent developments and future perspectives. Journal of Materials Chemistry C, 2021, 9, 11059-11078.	2.7	30
98	Stabilization of Orthorhombic CoSe ₂ by 2D-rGO/MWCNT Heterostructures for Efficient Hydrogen Evolution Reaction and Flexible Energy Storage Device Applications. ACS Applied Energy Materials, 2021, 4, 11386-11399.	2.5	30
99	Promising 2D/2D MoTe ₂ /Ti ₃ C ₂ T _{<i>x</i>} Hybrid Materials for Boosted Hydrogen Evolution Reaction. ACS Applied Energy Materials, 2021, 4, 11886-11897.	2.5	29
100	Unusual morphologies of reduced graphene oxide and polyaniline nanofibers-reduced graphene oxide composites for high performance supercapacitor applications. RSC Advances, 2014, 4, 22551-22560.	1.7	28
101	Improved Nonenzymatic Glucose Sensing Properties of Pd/MnO ₂ Nanosheets: Synthesis by Facile Microwave-Assisted Route and Theoretical Insight from Quantum Simulations. Journal of Physical Chemistry B, 2018, 122, 7636-7646.	1.2	28
102	High-rate quasi-solid-state hybrid supercapacitor of hierarchical flowers of hydrated tungsten oxide nanosheets. Electrochimica Acta, 2021, 366, 137389.	2.6	28
103	Temperature-dependent phonon dynamics of supported and suspended monolayer tungsten diselenide. AIP Advances, 2019, 9, .	0.6	27
104	Enhanced electron field emission from NiCo ₂ O ₄ nanosheet arrays. Materials Research Express, 2015, 2, 095011.	0.8	26
105	Vapour–liquid–solid growth of one-dimensional In ₂ Se ₃ nanostructures and their promising field emission behaviour. RSC Advances, 2015, 5, 65274-65282.	1.7	25
106	Glucose sensing and low-threshold field emission from MnCo ₂ O ₄ nanosheets. RSC Advances, 2016, 6, 29734-29740.	1.7	25
107	Field emission investigations of RuO2-doped SnO2 wires. Applied Surface Science, 2007, 253, 9159-9163.	3.1	24
108	Impedimetric humidity sensor based on α-Fe ₂ O ₃ nanoparticles. International Journal of Higher Education Management, 2015, 1, 88-92.	1.0	24

#	Article	lF	CITATIONS
109	Wide band gap and conducting tungsten carbide (WC) thin films prepared by hot wire chemical vapor deposition (HW-CVD) method. Materials Letters, 2016, 183, 315-317.	1.3	24
110	Development of pristine and Au-decorated Bi ₂ O ₃ /Bi ₂ WO ₆ nanocomposites for supercapacitor electrodes. RSC Advances, 2019, 9, 32573-32580.	1.7	23
111	Low threshold field electron emission from solvothermally synthesized WO2.72 nanowires. Applied Physics A: Materials Science and Processing, 2010, 98, 751-756.	1.1	22
112	Exfoliated 2D black phosphorus nanosheets: Field emission studies. Journal of Vacuum Science and Technology B:Nanotechnology and Microelectronics, 2016, 34, 041803.	0.6	22
113	Effect of plasma treatment on multilayer graphene: X-ray photoelectron spectroscopy , surface morphology investigations and work function measurements. RSC Advances, 2016, 6, 48843-48850.	1.7	22
114	Temperature and pressure dependent Raman spectroscopy of plasma treated multilayer graphene nanosheets. Diamond and Related Materials, 2018, 84, 146-156.	1.8	22
115	Fiber optic Fabry–Perot interferometer sensor: an efficient and fast approach for ammonia gas sensing. Journal of the Optical Society of America B: Optical Physics, 2019, 36, 684.	0.9	22
116	Synthesis of LaB6 micro/nano structures using picosecond (Nd:YAG) laser and its field emission investigations. Applied Physics A: Materials Science and Processing, 2009, 97, 905-909.	1.1	21
117	Temperature-dependent phonon shifts in atomically thin MoTe2 nanosheets. Applied Materials Today, 2016, 5, 98-102.	2.3	21
118	Enhanced field emission performance of NiMoO4 nanosheets by tuning the phase. Applied Surface Science, 2017, 418, 270-274.	3.1	21
119	High-performance dual cavity-interferometric volatile gas sensor utilizing Graphene/PMMA nanocomposite. Sensors and Actuators B: Chemical, 2020, 312, 127921.	4.0	21
120	Highly ordered nano-tunnel structure of hydrated tungsten oxide nanorods for superior flexible quasi-solid-state hybrid supercapacitor. Applied Surface Science, 2021, 545, 149044.	3.1	21
121	A single In-doped SnO2submicrometre sized wire as a field emitter. Journal Physics D: Applied Physics, 2007, 40, 3644-3648.	1.3	20
122	Surface modification of aligned CdO nanosheets and their enhanced field emission properties. RSC Advances, 2016, 6, 41261-41267.	1.7	20
123	High-performance field emission device utilizing vertically aligned carbon nanotubes-based pillar architectures. AIP Advances, 2018, 8, .	0.6	20
124	Bessel's polynomial fitting for electrospun polyacrylonitrile/polyaniline blend nanofibers based ammonia sensor. Materials Letters, 2018, 221, 70-73.	1.3	20
125	Experimental and density functional theory investigations of catechol sensing properties of ZnO/RGO nanocomposites. Applied Surface Science, 2019, 495, 143588.	3.1	20
126	Synthesis and characterization of LaB6 thin films on tungsten, rhenium, silicon and other substrates and their investigations asÂfield emitters. Applied Physics A: Materials Science and Processing, 2011, 104, 677-685.	1.1	19

#	Article	IF	CITATIONS
127	Synthesis of a 3D free standing crystalline NiSe _x matrix for electrochemical energy storage applications. Dalton Transactions, 2019, 48, 16873-16881.	1.6	18
128	MoS ₂ nanoparticles and h-BN nanosheets from direct exfoliation of bulk powder: one-step synthesis method. Materials Research Express, 2014, 1, 035038.	0.8	17
129	A back-to-back MOS–Schottky (Pt–SiO2–Si–C–Pt) nano-heterojunction device as an efficient self-powered photodetector: one step fabrication by pulsed laser deposition. Nanoscale, 2014, 6, 3550.	2.8	17
130	Photosensitive field emission study of SnS2 nanosheets. Journal of Vacuum Science and Technology B:Nanotechnology and Microelectronics, 2015, 33, 03C106.	0.6	17
131	Realization of Efficient Field Emitter Based on Reduced Graphene Oxideâ€Bi ₂ S ₃ Heterostructures. Physica Status Solidi (A) Applications and Materials Science, 2019, 216, 1900121.	0.8	17
132	Stable Field Emission from Layered MoS ₂ Nanosheets in High Vacuum and Observation of 1/f Noise. Nanomaterials and Nanotechnology, 2015, 5, 10.	1.2	16
133	Enhanced Antifungal Activity of WS ₂ /ZnO Nanohybrid against <i>Candida albicans</i> . ACS Biomaterials Science and Engineering, 2020, 6, 6069-6075.	2.6	16
134	Thermally Driven High-Rate Intercalated Pseudocapacitance of Flower-like Architecture of Ultrathin Few Layered δ-MnO ₂ Nanosheets on Carbon Nano-Onions. ACS Applied Energy Materials, 2020, 3, 11398-11409.	2.5	16
135	Raman spectroscopic investigations of the selenization of MoO3 in the chemical vapor deposition process to form two-dimensional MoSe2. Applied Surface Science, 2021, 538, 147946.	3.1	16
136	Functional Monochalcogenides: Raman Evidence Linking Properties, Structure, and Metavalent Bonding. Physical Review Letters, 2020, 125, 145301.	2.9	15
137	TiO ₂ nanoflowers based humidity sensor and cytotoxic activity. RSC Advances, 2020, 10, 29378-29384.	1.7	15
138	Raman Fingerprint of Pressure-Induced Phase Transitions in TiS ₃ Nanoribbons: Implications for Thermal Measurements under Extreme Stress Conditions. ACS Applied Nano Materials, 2020, 3, 8794-8802.	2.4	15
139	Arc plasma synthesized LaB6 nanocrystallite film on various substrates as a field emitter. Journal of Nanoparticle Research, 2010, 12, 2393-2403.	0.8	14
140	Low frequency noise and photo-enhanced field emission from ultrathin PbBi ₂ Se ₄ nanosheets. Journal of Materials Chemistry C, 2016, 4, 1096-1103.	2.7	14
141	Spatially branched CdS–Bi ₂ S ₃ heteroarchitecture: single step hydrothermal synthesis approach with enhanced field emission performance and highly responsive broadband photodetection. RSC Advances, 2016, 6, 95092-95100.	1.7	13
142	Fabrication of In-doped SnO ₂ nanowire arrays and its field emission investigations. Journal of Experimental Nanoscience, 2010, 5, 527-535.	1.3	12
143	Single-layer graphene doping through molecular interaction: field-effect transistor and atomic force microscopy investigations. International Journal of Higher Education Management, 2015, 1, 52-58.	1.0	12
144	Enhanced field emission from hexagonal rhodium nanostructures. Applied Physics Letters, 2008, 92, 253106.	1.5	11

#	Article	IF	CITATIONS
145	Field emission investigation of single Fe-doped SnO2 wire. Solid State Sciences, 2009, 11, 1114-1117.	1.5	11
146	Observation of enhanced field emission properties of Au/TiO2 nanocomposite. Applied Physics A: Materials Science and Processing, 2016, 122, 1.	1.1	11
147	Humidity and H ₂ O ₂ sensing behavior of Te nanowires. International Journal of Higher Education Management, 2016, 2, 8-14.	1.0	11
148	Synthesis of γâ€WO ₃ thin films by hot wire VD and investigation of its humidity sensing properties. Physica Status Solidi (A) Applications and Materials Science, 2017, 214, 1600717.	0.8	11
149	Quasi-one-dimensional van der Waals TiS3 nanosheets for energy storage applications: Theoretical predications and experimental validation. Applied Physics Letters, 2022, 120, .	1.5	11
150	Microwaveâ€Assisted Synthesis of Few‣ayered TaTe ₂ and Its Application as Supercapacitor. European Journal of Inorganic Chemistry, 2015, 2015, .	1.0	10
151	Surface chemical bonds, surface-enhanced Raman scattering, and dielectric constant of SiO2 nanospheres <i>in-situ</i> decorated with Ag-nanoparticles by electron-irradiation. Journal of Applied Physics, 2016, 120, .	1.1	10
152	Field emission properties of highly ordered low-aspect ratio carbon nanocup arrays. RSC Advances, 2016, 6, 9932-9939.	1.7	10
153	Borophene: Freestanding Borophene and Its Hybrids (Adv. Mater. 27/2019). Advanced Materials, 2019, 31, 1970196.	11.1	10
154	MoWS ₂ nanosheets incorporated nanocarbons for high-energy-density pseudocapacitive negatrode material and hydrogen evolution reaction. Sustainable Energy and Fuels, 2022, 6, 2941-2954.	2.5	10
155	Low turn-on field and high field emission current density from Ag/TiO2 nanocomposite. Chemical Physics Letters, 2016, 657, 167-171.	1.2	9
156	Synthesis and self-assembly of dumbbell shaped ZnO sub-micron structures using low temperature chemical bath deposition technique. Materials Chemistry and Physics, 2016, 169, 152-157.	2.0	9
157	Inhibition of Quorum Sensing, Motility and Biofilm Formation of Pseudomonas aeruginosa by Copper Oxide Nanostructures. Journal of Cluster Science, 2021, 32, 1531-1541.	1.7	9
158	Solvothermal Growth of PbBi ₂ Se ₄ Nanoâ€Flowers: A Material for Humidity Sensor and Photodetector Applications. Physica Status Solidi (A) Applications and Materials Science, 2019, 216, 1900065.	0.8	8
159	Tuning the synergistic effects of MoS ₂ and spinel NiFe ₂ O ₄ nanostructures for high performance energy storage and conversion applications. Sustainable Energy and Fuels, 2021, 5, 3906-3917.	2.5	8
160	Enrichment of the field emission properties of NiCo ₂ O ₄ nanostructures by UV/ozone treatment. Materials Advances, 2021, 2, 2658-2666.	2.6	8
161	Tunable light emission from chemical vapor deposited two-dimensional MoSe2 by layer variation and S incorporation. Journal of Vacuum Science and Technology A: Vacuum, Surfaces and Films, 2020, 38, .	0.9	8
162	RuO2 doped SnO2 nanobipyramids on Si (100) as a field emitter. Thin Solid Films, 2008, 516, 6388-6391.	0.8	7

#	Article	IF	CITATIONS
163	Fundamentals and Properties of 2D Materials in General and Sensing Applications. , 2019, , 5-24.		7
164	Ultra-high energy stored into multi-layered functional porous carbon tubes enabled by high-rate intercalated pseudocapacitance. Carbon, 2022, 192, 153-161.	5.4	7
165	Enhanced van-der Waals separation in hydrated tungsten oxide nanoplates enables superior pseudocapacitive charge storage. Journal of Alloys and Compounds, 2022, 914, 165227.	2.8	7
166	Preparation of Exfoliated Bi[sub 2]Te[sub 3] Thin Films. , 2011, , .		6
167	Architecture of 2D MoS2 nanosheets and 3D CdMoS4 marigold flowers: Consequence of annealing on field emission performance. Microporous and Mesoporous Materials, 2016, 225, 573-579.	2.2	6
168	A Facile Approach towards Fabrication of GdB6-ZnO Heteroarchitecture as High Current Density Cold Cathode. ChemistrySelect, 2016, 1, 3723-3729.	0.7	5
169	Enhanced Field Emission Characteristics of a 3D Hierarchical HfO2-ZnO Heteroarchitecture. ChemistrySelect, 2017, 2, 2305-2310.	0.7	5
170	Enhanced Field Emission Performance of MoO ₃ Nanorods and MoO ₃ â€rGO Nanocomposite. ChemistrySelect, 2017, 2, 10912-10917.	0.7	5
171	Pulsed laser-deposited nanocrystalline GdB6 thin films on W and Re as field emitters. Applied Physics A: Materials Science and Processing, 2016, 122, 1.	1.1	4
172	Extraction of the Very High Tunneling Current and Extremely Stable Emission Current from GdB ₆ /W‶ip Source Synthesized Using Arc Plasma. ChemistrySelect, 2017, 2, 562-566.	0.7	4
173	Nonlinear Fowler-Nordheim behavior of a single SnO2nanowire. Journal of Vacuum Science and Technology B:Nanotechnology and Microelectronics, 2017, 35, 02C105.	0.6	4
174	Future Prospects of 2D Materials for Sensing Applications. , 2019, , 481-482.		4
175	PVA-coated miniaturized flexible fiber optic sensor for acetone detection: a prospective study for non-invasive diabetes diagnosis. Journal of Materials Science: Materials in Electronics, 2022, 33, 2509-2517.	1.1	4
176	PbS Nanostarâ€Like Structures as Field Emitters. ChemistrySelect, 2017, 2, 5175-5179.	0.7	3
177	Highly stable field emission from micron sized homogeneous β-Ga2O3 sheets grown using vapor phase transport route. Materials Chemistry and Physics, 2020, 254, 123512.	2.0	3
178	MoS ₂ and CdMoS ₄ nanostructure-based UV light photodetectors. Nanoscale Advances, 2021, 3, 4799-4803.	2.2	3
179	Efficient humidity sensor based on surfactant free Cu2ZnSnS4 nanoparticles. Ceramics International, 2022, 48, 28898-28905.	2.3	3
180	A Perspective on Atomically Thin 2D Inorganic Layered Materials for Biosensor. Journal of Nanomedicine Research, 2014, 2, .	1.8	2

#	ARTICLE	IF	CITATIONS
181	Field emission investigations on an array of LaB6 micro/nanostructures obtained using picosecond (Nd:YAG) laser treatment. , 2009, , .		1
182	Enhancement in the field emission behavior of graphene in N <inf>2</inf> /O <inf>2</inf> high vacuum ambience. , 2014, , .		1
183	High performance single crystalline PbWO4 nanorod field effect transistor. Journal of Materials Science: Materials in Electronics, 2015, 26, 10044-10048.	1.1	1
184	Black phosphorous nanosheets: Prospective field emitter. , 2015, , .		1
185	Graphene nanosheets assisted carbon hollow cylinder for high-performance field emission applications. Materials Research Express, 2019, 6, 095066.	0.8	1
186	Field Emission from Nanocrystalline LaB6 Prepared by Laser Ablation. , 2006, , .		0
187	Enhanced Field Emission Characteristics of Novel ZnO Multipod Nanostructures. , 2006, , .		0
188	Photosensitive field emission study of SnS <inf>2</inf> nanosheets. , 2014, , .		0
189	One-pot thermal evaporation synthesis of CdS-RGO hetrostructure and its field emission study. , 2015, , .		Ο
190	Transition metal di-chalcogenides and their nanocomposite prospective field emitters. , 2015, , .		0
191	Single SnO <inf>2</inf> nanowire: Field emission investigations. , 2016, , .		0
192	Field emission investigation of composites of Polypyrrole with graphene oxide, reduced graphene oxide and graphene nanoribbons. , 2016, , .		0
193	Photo Sensor Based on 2D Materials. , 2019, , 465-479.		Ο
194	Structure and properties of 2D materials in general and their importance to energy storage. , 2021, , 11-75.		0
195	Electrical characterization of pulsed laser deposited high-k HfO2 nanoparticles on tapered Cu2O nanowires: promising cold cathode applications. Journal of Materials Science: Materials in Electronics, 2021, 32, 8440-8449.	1.1	0
196	Spectroscopic probe of atomically thin domains of CVD-grown MoSe2. AIP Conference Proceedings, 2020, , .	0.3	0
197	PtSe2 Nanosheets as Efficient Field Emitter. , 2021, , .		0